ENGINEER - Vol. LV, No. 01, pp. [49-61], 2022

DOI: http://doi.org/10.4038/engineer.v55i1.7486

Assessment of Time-dependent Temperature Behaviour in Immature Concrete Walls using Numerical Analysis

H.P. Rathnayaka, D.K.A.M.P. Dassanayake and H.D. Yapa

Abstract: Hydration of cement is exothermic and the consequent temperature development leads to non-structural cracking in immature concrete. The maximum internal temperature drop (T_1) is a governing parameter towards thermal cracking, and for structural deigns, T_1 values recommended in the codes of practice are commonly used. Past investigations show that such recommendations could be too conservative. Amid the complexity of concrete thermal behaviour, one good prediction option is to use numerical methods. In this light, this study attempted to formulate recommendations for T_1 via finite element (FE) analysis. First, a commercial FE software was validated for two distinct experimental results and, second, the FE application was used to predict the temperature in concrete walls. The variables were: wall thickness (300 - 1000 mm); cement composition (350 - 560 kg/m^3); and plywood/steel formwork types. Semi-adiabatic experiments were conducted to obtain the rate of heat evolution in concrete. The numerical results showed that the predicted T_1 values were considerably lower than those recommended in two currently practiced guidelines. The observed disparity was in the range of 22% - 34%. It was also shown that T_1 could be further reduced by about 15% and 23.5% through supplementing the mixes with fly ash by 20% and 35%, respectively.

Keywords: Early-age thermal cracking; Finite element analysis; Heat-loss compensation; Heat of hydration; Semi-adiabatic experiment

1. Introduction

Cement hydration is significantly exothermic, and consequently, mass concrete construction confronts with undesirable internal temperature development. On the one hand, high temperature is adverse for concrete, for instance, temperature beyond 70 °C could be a cause of severe material deterioration due to delayed ettringite formation [1]. On the other hand, because of low thermal conductivity of concrete, the heat generation leads to internal temperature gradients which could cause undesirable cracking in immature concrete [2]. Also, in externally restrained structures, the drop of temperature during the cooling phase contracts concrete, and consequently, through cracking is possible [3]. It is therefore vital to take appropriate measures to control temperature development in concrete. Popular temperature controlling methods used in the construction industry are the use of low-heat cement, use of pre-cooling methods (e.g. use of chilled water) and use of post-cooling methods (e.g. installation of internal pipe cooling networks). Also, the use of proper curing methods is essential for mitigating thermal cracking in concrete [2].

In order to identify the need for temperature controlling for a concrete structure, it is useful to forecast the state of temperature. However, that is a challenge because temperature development of concrete depends on many parameters, including: heat evolution of concrete; internal thermal conduction; thermal conduction into previously cast concrete or to foundations; convection at the boundaries; concrete specific heat; radiation, etc. [4]. Also, heat transfer of concrete involves a number of inter-related mechanisms where none of which has a closed-form solution. Hence the use of numerical approaches of Finite Element (FE) and Finite Difference (FD) methods have become popular as a temperature prediction tool for concrete structures [5]. In contrast to the FD option, the FE method has more merits in

Eng. H.P. Rathnayaka, AMIE (Sri Lanka), B.Sc. Eng. (Hons) (Peradeniya), MSc Eng. (Peradeniya)
Email:harshanasoftnet@gmail.com
https://orcid.org/0000-0003-4230-1576
Eng. D.K.A.M.P. Dasanayake, C.Eng, MIE(Sri Lanka), B.Sc. Eng. (Hons) (Peradeniya), MSc Eng. (Peradeniya), Civil Engineer, Airport & Aviation Services Sri Lanka (Private) Limited.
Email:mpddasanayake@gmail.com
https://orcid.org/0000-0002-1888-7557
Eng. (Dr.) H.D. Yapa, AMIE (Sri Lanka), B.Sc. Eng. (Hons) (Moratuwa), Ph.D. (Cantab), Senior Lecturer, Department of Civil Engineering, University of Peradeniya.
Email:hdy@pdn.ac.lk
https://orcid.org/0000-0002-7213-5276

terms of dealing with sophisticated problems including: irregular geometries; diverse boundary conditions; construction patterns, etc. [6].

The key parameter pertaining to crack controlling of restrained concrete structures is the maximum drop of temperature (T_1) from the peak temperature of the structure [7], see Figure 1. This may be governed by several parameters including cement content, structure thickness, type of formwork, etc. As previously mentioned, a detailed temperature simulation is to be conducted for precise estimation of such temperature, however, the codes of practice provide simplified guidelines for this purpose [3, 8-10]. However, some recent investigations show that the temperature levels anticipated by such codes could be too conservative to be used in the local context [11]. Accordingly, Mataraarachchi et al. [12] recommended some guidelines for selection of T_1 where scope was limited to cement contents of 380 kg/m^3 and 400 kg/m^3. In this light, this study was implemented with the intention of exploring the appropriateness of T_1 values stipulated in the British and Eurocodes for a wide concrete strength range (or cement content range). First a numerical model was developed and validated on available experimental results. Second, the model was used to obtain temperature predictions. Two semi-adiabatic experiments were also conducted to estimate the heat evolution of concrete.

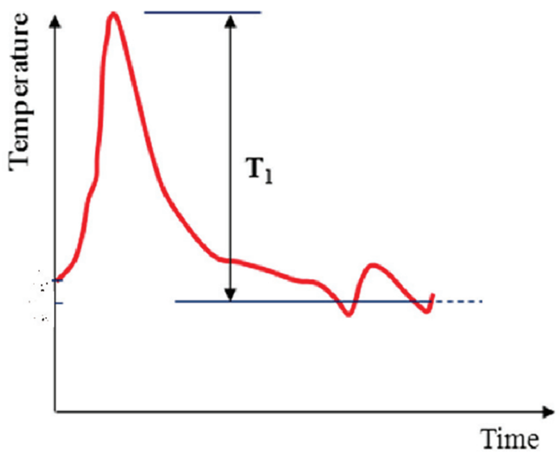

Figure 1 – T_1 Definition

2. Literature Survey

The literature survey was conducted with the focus on existing concrete crack controlling guidelines, past concrete temperature assessment investigations, and heat of hydration assessment methods for concrete.

2.1 Crack Controlling Guidelines

BS 8007 was the popular code of practice that covered guidelines towards early-age thermal crack controlling for concrete structures [8]. It has now been superseded by Eurocode 2 [9, 10]. Besides, CIRIA C660 [3] is a complementary document for Eurocode 2 that provides detailed information on crack controlling for concrete structures [7]. All these packages are based on the fundamental concept that when a restrained concrete is subjected to a temperature drop of T_1 (due to cooling subsequent to the peak temperature), the concrete is subjected to a thermal strain of,

$$\varepsilon = R\alpha T_1 \qquad \ldots (1)$$

where, α is the coefficient of thermal expansion of concrete and R is a factor that represents the restraint conditions of the structural system. BS 8007 expressed T_1 for cement contents in the range of 325 – 400 kg/m^3 at the background of 15 °C mean daily temperature and 20 °C concrete placing temperature. However, the climate conditions in Sri Lanka are completely different to those found in the above mentioned literature. Mostly, the local ambient temperature may vary around 28 °C and the concrete placing temperature could be slightly above that [12]. In order to account such climatic differences, the Sri Lankan practice had been to add 8 °C to BS 8007 T_1 values [11].

The approach in CIRIA C660 [3] to estimate T_1 is more detailed than BS 8007 where provisions are available to include widespread input variables via spreadsheets. For instance, for the conditions of 32 °C placing temperature, 30 °C mean ambient temperature, 1132.6 J/kg°C specific heat, 2.52 W/m°C thermal conductivity, formwork thermal conductivity of 5.2 W/m^2 °C for plywood, 3.5 m/s wind speed, cement contents of 350 kg/m^3, 400 kg/m^3 and 550 kg/m^3, T_1 predictions from CIRIA C660 are tabulated in Table 1.

Table 1 – Typical Values for T_1 (°C) Calculated from CIRIA C660 (Bamforth, 2007)

Wall thickness	Plywood		
	350 kg/m^3	400 kg/m^3	550 kg/m^3
300 mm	33.8	38.8	53.4
500 mm	40.1	45.9	63.3
700 mm	43.9	50.4	69.3
1000 mm	47.8	54.4	74.9

2.2 Experimental Evidence on T_1

A laboratory investigation was carried out by Nanayakkara & Wannigama [11] to assess the validity of recommended T_1 in BS 8007. The temperature rise in 300 mm, 500 mm, 700 mm and 1000 mm thick, 1200 mm high and 1200 mm long concrete wall panels was monitored via thermo-couples placed in each panel as shown in Figure 2(a). A 12 mm thick plywood formwork was used at each side. The wall concrete comprised of a 400 kg/m^3 cement (OPC) content. The mean daily temperature and the placing temperature of the concrete were 30 °C and 32 °C, respectively. More details about the experiment can be found from Nanayakkara & Wannigama [11].

It was concluded that the experimental T_1 values were considerably lower than the prediction from BS 8007 whereas one would expect the vice versa because the experimental placing temperature and mean daily temperature were higher than the conditions associated in BS 8007. Figure 2(b) shows this comparison and it includes the predictions from the CIRIA C660 approach as well. Interestingly, except for the 300 mm thickness, the two prediction approaches provide reasonably similar T_1 values.

2.3 Numerical Investigation on T_1

Mataaarachchi et al. [12] conducted a numerical investigation into estimating T_1 applicable for the local conditions. Herein, a multi component cement hydration model was used to introduce heat of hydration of concrete to a finite element model and T_1 predictions for different wall thicknesses (300 mm – 1000 mm) at cement contents of 380 kg/m^3 and 400 kg/m^3 were obtained. It was concluded that, except for 300 mm wall, T_1 values provided in BS 8007 were higher than the obtained values. It therefore fairly verified the experimental observations of Nanayakkara & Wannigama [11].

2.4 Adiabatic Behaviour of Concrete

The adiabatic temperature behaviour of concrete is a crucial parameter for concrete temperature simulation. It represents heat evolution of concrete. Various experimental methods such as the heat solution method, adiabatic calorimeter method and semi-adiabatic calorimeter method are available to quantify the adiabatic temperature profile [13-16]. Amongst these methods, the most precise approach is the adiabatic calorimetric approach [13] which relies on the principle that, at any time during the test, the temperature of the sample surroundings must be equal to the temperature of the concrete. Hence, additional heat must be supplied from outside to maintain the adiabatic conditions and the approach is therefore rather sophisticated and expensive [17].

As an alternative to the adiabatic experiment, the use of semi-adiabatic test and prediction of the pertaining adiabatic behaviour via heat loss estimation has been identified possible [17, 18]. The validity and the accuracy of this approach have been sufficiently verified [17]. Figure 3(a) shows a typical adiabatic and semi-adiabatic profile correlation for concrete.

2.5 Semi Adiabatic Test Setup

Different versions of semi-adiabatic curing test setups have been developed, Figure 3(b) shows schematic diagram of a typical apparatus. Herein, the concrete sample is placed in the internal polystyrene chamber, and in order to reduce the heat loss, it is placed in a larger box and the gap is filled with polystyrene bubbles. Thermocouples are used to record the temperature. The amount of heat loss depends on the specimen size and the effectiveness of the heat insulation provided. Smaller the loss, more accurate is the adiabatic temperature estimation. Also, the error occurring in heat loss computation is larger for small specimens [17].

2.6 Heat Loss Compensation Technique

As proposed by Ng et al. [17], for a specimen of volume V, the difference between adiabatic temperature rise T_G and the measured temperature rise (equivalent to the difference of volumetric mean temperature of concrete T_V and placing concrete temperature T_P) is found from the following equation.

$$T_G - (T_V - T_P) = \frac{H_L}{V\psi} \qquad \dots (2)$$

where, H_L is the heat loss and ψ is the volumetric specific heat capacity of concrete.

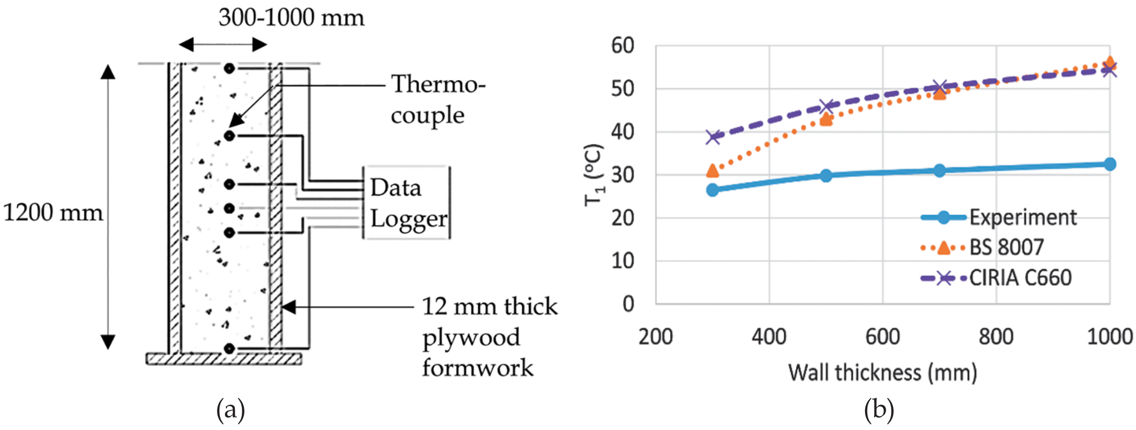

Figure 2 – Nanayakkara and Wannigama (2003) Study: (a) Experimental Setup; (b) Comparison with Experimental Temperature Predictions

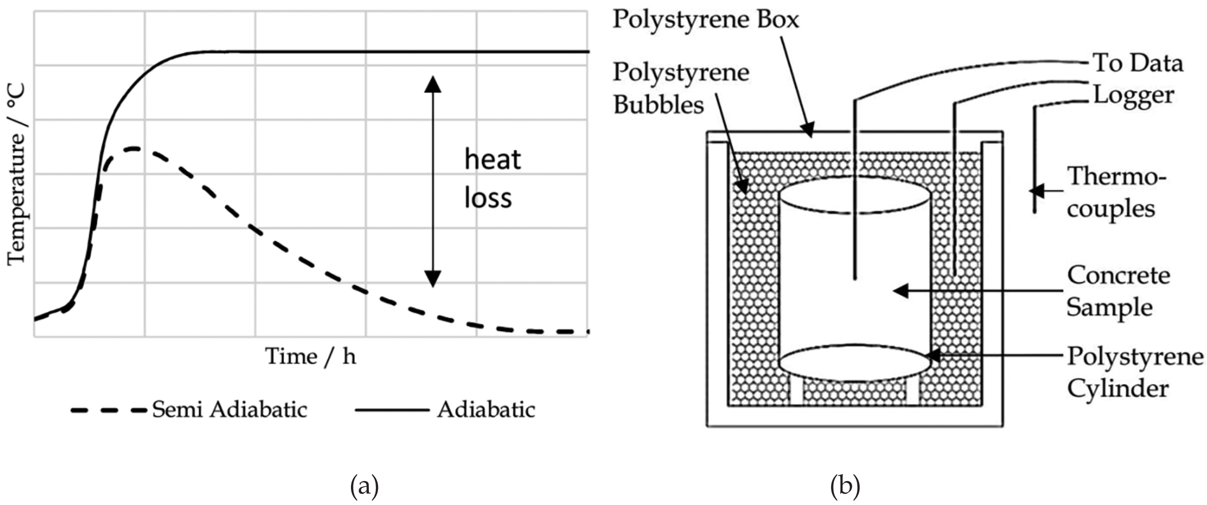

Figure 3 – (a) Semi-Adiabatic Profile; (b) Semi Adiabatic Test Apparatus

When k is the overall thermal conductivity of the insulating system, it is possible to express the heat loss as,

$$H_L = \int_0^t k(T_S - T_A)dt \qquad \text{... (3)}$$

where, T_S is the surface mean temperature of the concrete, T_A is the ambient temperature, and t is the time after placing concrete. By rearranging Eqs. (2) and (3), the adiabatic temperature can be expressed in the form of Eq. 4.

$$T_G = (T_V - T_P) + \frac{1}{V\psi} \int_0^t k(T_S - T_A)dt \qquad \text{... (4)}$$

Since k, V and ψ are constants for a selected semi-adiabatic test setup and a concrete mix, the formulation can be simplified with the substitution of $\lambda = k/V\psi$. When sufficiently small time interval Δt_i is considered, Eq. 3 can then be converted to the numerical form of Eq. 5.

$$T_G = (T_V - T_P) + \lambda \sum (T_S - T_A)\Delta t_i \qquad \text{... (5)}$$

Beyond 120 hours, heat evolution becomes fairly negligible, and therefore $T_G = 0$. Accordingly, λ can be calculated from:

$$\lambda = - \frac{(\partial T_V / \partial t)}{(T_S - T_A)} \qquad \text{... (6)}$$

A time interval of five minutes has been identified to be appropriate for the procedure [17].

When the temperature is measured at four points within a cube where T_m is temperature of center of mass, T_f is temperature of center of face, T_e is temperature of mid-point of edge and T_c is temperature of corner, T_V and T_S can be represented in the form of [18]:

$$T_V = \frac{64}{125}T_m + \frac{48}{125}T_f + \frac{12}{125}T_e + \frac{1}{125}T_c \quad \text{... (7)}$$

$$T_S = \frac{16}{25}T_f + \frac{8}{25}T_e + \frac{1}{25}T_c \quad \text{... (8)}$$

If the sample is small, one-point temperature measurement can be adopted, and in that case, the central temperature measurement represents both T_V and T_S [17].

3. Experimental Investigation

The adiabatic temperature behaviour is essential information for the intended temperature simulation of this study. Wasala & Yapa [19] conducted a series of semi adiabatic experiments targeting the 40 – 50 MPa compressive strength range and they were used to represent normal strength concrete. In order to cover high strength concrete, two further semi-adiabatic experiments at w/c ratios of 0.30 and 0.40 were conducted in this study. In addition, to facilitate FE model verification against an available pile cap mock-up model, another semi-adiabatic experiment to associate the concrete mix of that context was also conducted.

3.1 Concrete Mix Design

The concrete mix designs are shown in Table 2 and it includes the new mixes (M1, M2), three mixes from the Wasala & Yapa [19] study (M3, M4, M5), and the mix used for model verification (M6). Of note is that the two numerals in M1 – M5 mix designations indicate cement and fly ash contents, respectively. The table also shows the 28-day cube strength results and the initial concrete temperature. Matharaarachchi et al. [12] explained that the heat evolution is sensitive to the cement composition (particularly to C_3A and C_2A) as well as to the fineness. However, that was not considered in this study.

3.2 Semi-Adiabatic Experiment

The test setup consisted of a polystyrene 180 mm cubical container, plastic insulation sheet, polystyrene bubbles and a 450 mm polystyrene square box, see Figure 4.

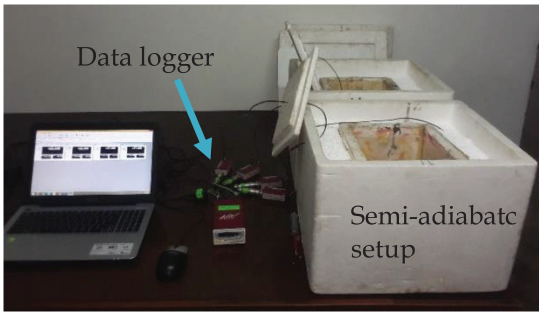

Figure 4 – Semi-adiabatic Setup

Table 2 – Concrete Mix Proportions for 1 m³ Concrete

Notation	M1-560	M2-420	M3-379-95	M4-353-190	M5-349	M6
W/C	0.30	0.40	0.50	0.52	0.46	0.42
OPC (kg)	560	420	379	353	350	330
Fly Ash (kg)	0	0	95	190	0	110
Water (kg)	168	168	191	184	162	185
Fine Agg. (kg)	535	544	742	958	958	431
Quarry Dust (kg)	-	-	-	-	-	185
Coarse Agg. (kg)	1137	1268	998	998	997	1197
Admixture (l)	5.6	4.2	0.0	0.0	3.5	5.005
Avg. Cube Strength (MPa)	71.6	61.6	49.5	49.0	44.5	50.0
Initial Temp (°C)	30.6	31.1	28.0	26.3	26.5	26.8

The concrete was cast inside the polyester cube and that was placed in the large polyester container. The plastic sheet was placed at the concrete/polyester interface and the gap between the two containers was filled with the polystyrene bubbles. One thermocouple was used at the middle of the concrete cylinder and another was used to monitor the ambient temperature. The thermocouples were connected to a data logger to record the temperature. Upon collecting readings for about 140 hrs., the experiments were terminated and the data was used to plot semi adiabatic profiles to compute λ, and to predict the adiabatic behaviours. The Arrhenius maturity relationship was utilised to convert the adiabatic profiles to the required initial temperature of concrete [20], 2003). At this conversion, the activation energy parameter (E) was assumed to be 33.5 kJ/mol based on guidelines found in the literature [21].

4. Numerical Modelling

With the intention of assessing the validity of existing guidelines on estimating T_1, a 3-dimensional (3D) FE modelling series was conducted. MIDAS FEA [22] software was used as the FE tool. First the tool was verified for two available experimental results, and second, it was used to identify T_1 values for typical RC wall constructions.

The major differential relationship implemented in MIDAS FEA is,

$$C\dot{T} + (K + H)T = F_Q + F_q \quad ...(9)$$

where,

$$C\text{ (mass)} = \left[\int_V \rho c N_i N_j dxdydz \right] \quad ...(10)$$

$$K\text{ (conduction)} = \left[\int_V \left(k_{xx}\frac{\partial N_i}{\partial x}\frac{\partial N_j}{\partial x} + k_{yy}\frac{\partial N_i}{\partial y}\frac{\partial N_j}{\partial y} + k_{zz}\frac{\partial N_i}{\partial z}\frac{\partial N_j}{\partial z}\right) dxdydz \right] \quad ...(11)$$

$$H\text{ (convection)} = \left[\int_S h_c N_i N_j dS_h \right] \quad ...(12)$$

$$F_Q\text{(heat sourse load)} = \int_V N_i Q dxdydz \quad ...(13)$$

$$F_q\text{(heat flux load)} = -\int_S q N_i dS_q \quad ...(14)$$

where ρ is the density, c is the specific heat, $k_{xx,}$ k_{xx} and k_{xx} are heat conductivity in x, y and z directions, respectively, h_c is the convection coefficient, Q is the rate of heat flow, T is the nodal temperature and $N_{i,}N_j$ are shape functions.

The time dependent behaviour is formulated with the relation of,

$$\alpha\dot{T}_{i+1} + (1-\alpha)\dot{T}_i = \frac{T_{i+1} - T_i}{\Delta t_{i+1}} \quad ...(15)$$

where α is an integral variable to be between 0 and 1. The value was set to 0.5 in this study.

Table 3 summaries the thermal properties selected from the literature to use as input parameters for the FEA models. The selection was made based on the recommendations found in Ballim [2], Bamforth [3], Dissanayaka and Yapa [7]. In addition, as explained previously, the heat load (Q) was introduced to the software based on the semi-adiabatic experimental results.

5. Results and Discussion

5.1 Experimental Results

Figure 5 presents the experimental semi-adiabatic temperature profiles. Of note is the initial thermal behaviour of the current investigation mixes (M1, M2 and M6) and that of the mixes obtained from the literature (M3, M4 and M5) are slightly different. It could be attributed to the differences in OPC types and in the admixtures used. Exploration into such details is identified as a matter for future work.

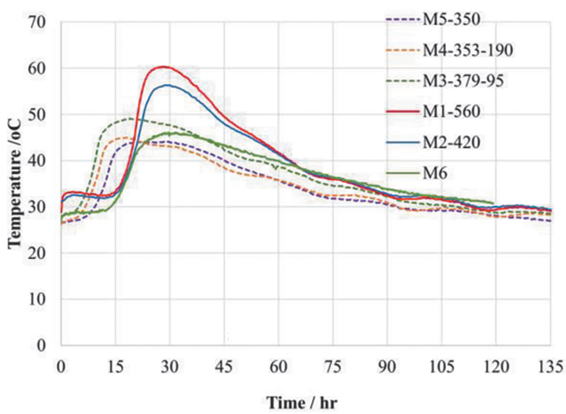

Figure 5 – Semi Adiabatic Temperature Profiles

Table 3 – Physical Parameters Selected for Numerical Modelling

Parameter	Values	Unit
Specific heat of concrete	0.025	kcal/kg°C
Weight density of concrete	2400	kg/m^3
Weight density of soil	1800	kg/m^3
Thermal conductivity of concrete	2.52	W/m.K
Coefficient of thermal expansion	1.0×10^{-5}	mm/mm°C
25 mm steel	18.9	W/m^2 °C
12 mm plywood	6.3	W/m^2 °C
18 mm plywood	5.2	W/m^2 °C
24 mm plywood convection	4.2	W/m^2 °C
37 mm plywood	3.2	W/m^2 °C
Saw dust convection	3.2	W/m^2 °C
Soil convection	12	W/m^2 °C
Expanded polystyrene	1.3	W/m^2 °C

Figure 6 shows the predicted adiabatic temperature profiles. The λ values pertaining to each situation were computed to be in the range of 0.0302 - 0.0366. As expected, a reasonable relationship is observed between the binder content and the temperature accumulation so that higher the binder content, higher is the adiabatic temperature.

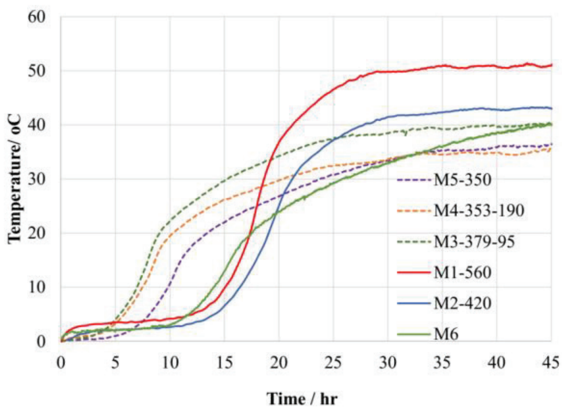

Figure 6 – Adiabatic Temperature Profiles

5.2 Numerical Model Verification

The FE model was verified for two experimental investigations.

Verification 1

The numerical model was validated on a mock-up test (in regard to a pump house construction) done in Sri Lanka. The mock-up section had dimensions of 1.4 m thickness (which was similar to the actual thickness of the pump house), 2 m length and 2 m width. The target concrete quality was C35A (exact mix proportions are shown for M6 in Table 2). Both the ambient temperature and the initial concrete temperature was 33 °C. Eleven thermocouples were located within the mock-up as shown in Figure 7. The locations have been selected to cover both the interior and the surface areas.

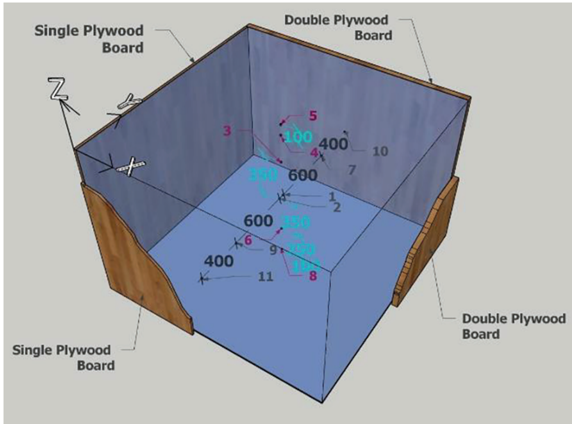

Figure 7 - Mock-up Test Thermocouple Locations (dimensions in mm)

Considering the symmetry of the mock-up, only a quarter of the structure was simulated in the FE model. Both concrete and soil were meshed with 200 mm solid elements, see Figure 8. In the quarter model, 2 m x 2 m x 1 m soil volume was included. It should be noted that the mesh size was selected based on a convergence test where the peak temperature prediction decreased with the refining of the mesh size from 1000 mm (T = 68.3 °C) to 200 mm (T = 67.9 °C) and was stable thereafter.

Convection boundary conditions were assigned to the outer concrete faces and to the top face, see Figure 8(a). Also, prescribed boundary conditions were applied around the soil mass to represent the constant temperature below the ground level. Symmetric support conditions were applied around two surfaces of the concrete block and soil mass to represent the quarter model, see Figure 8 (b). Except for the symmetric surfaces of the soil mass, pin support was applied for all the nodes. The heat parameters appropriate for this simulation were used from Table 3. As previously mentioned, a semi-adiabatic experiment was dedicated to represent this particular concrete mix (M6) and thereby the pertaining adiabatic profile was obtained, see Figures 4 and 5.

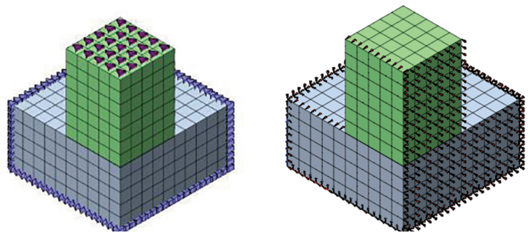

(a) (b)

Figure 8 - Boundary Conditions: (a) Convection; (b) Prescribed

Figures 9 (a) – (d) illustrate the comparisons between the experimental measurements and the FE predictions for distinct locations of the mock-up element. Interestingly, all the predictions were observed to be with high level of accuracy. Except for the bottom node, a slight under-prediction (max 5.5 ^{o}C, 7.5%) is generally observed. The time to reach the peak temperature was also predicted fairly accurately.

Verification 2

The laboratory experiment conducted by Nanayakkara and Wannigama [11] was tested for FE simulations. Of note is that this particular investigation comprised 400 kg/m^3 cement content whereas none of the available adiabatic profiles (presented in Figure 6) covered that composition. Hence, as an alternative, considering the correlation between the cement content and the heat of hydration, the average adiabatic behaviour of M2-420 and M5-350 was used as the adiabatic input for the FE model. The other modelling parameters were appropriately selected from Table 3.

Figure 10 compares the experimental and predicted temperatures and highlights that the prediction accuracy is reasonable. All the temperatures were slightly over-predicted and that margin increases with the increasing wall thickness. The maximum deviation was 7 ^{o}C. The figure also includes the estimations from the BS 8007 and CIRIA C660 approaches. As previously discussed, those estimations are far beyond the experimental values and this comparison points up the potential of the FE predictions over the code based predictions. Considering the current practice of adding 8 ^{o}C to the code based T_1 predictions for local construction [11], the same margin was added to the FE predictions and those are also shown in Figure 10. Interestingly, still the augmented FE predictions were below the code based estimations (except for BS 8007 prediction for 300 mm wall). This observation was useful in the formation of T_1 recommendations that are presented later in the paper.

Both model verifications thus showed good evidence on the potential of the FE model for concrete temperature prediction. In fact, verification 1 that was done on the mock-up test can be deemed as a comprehensive attempt because of the availability of temperature profile measurements at different locations and of the usage of the exact concrete mix to obtain the adiabatic temperature profile. The following points could be highlighted about the observed minor discrepancies during the validation.

a) The incapability of the used numerical tool to account for the concrete maturity behaviour could be the potential reason for the observed over-prediction for the laboratory experiment (verification 2).
b) Amid software shortcomings, solar radiation should have increased the temperature of the mock-up experiment whereas that was not accounted in the FE simulation. Hence, under-predictions from the FE model could be expected for such scenarios.
c) The correlation for the bottom temperature in the mock-up test showed a better precision than for the other locations (Figure 9 (c)). Since the solar ration influence is to be minimal to the bottom region of the concrete, such a behaviour is explainable.

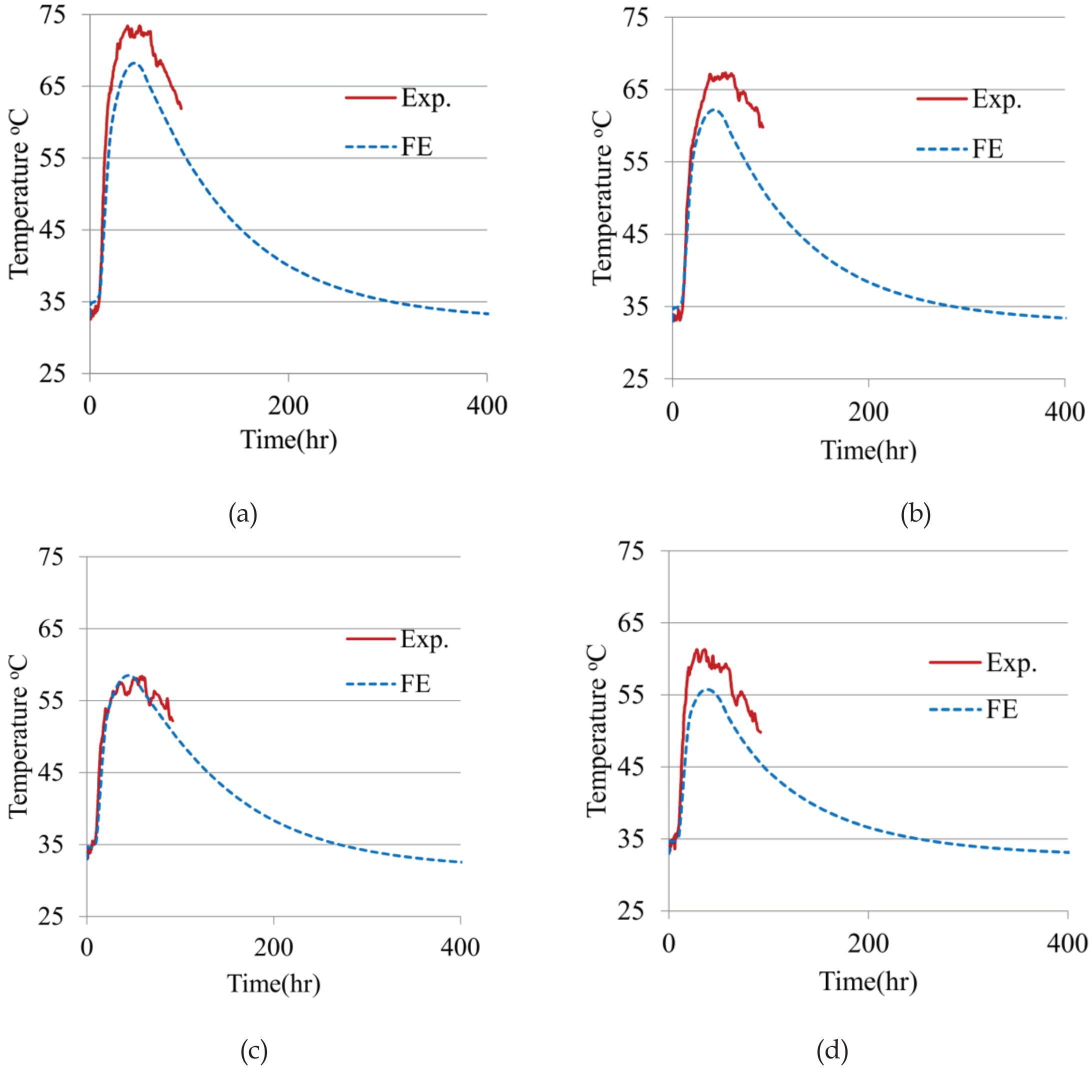

Figure 9 - Temperature Comparisons for Thermocouples of: (a) 1 and 2; (b) 4; (c) 8; (d) 10

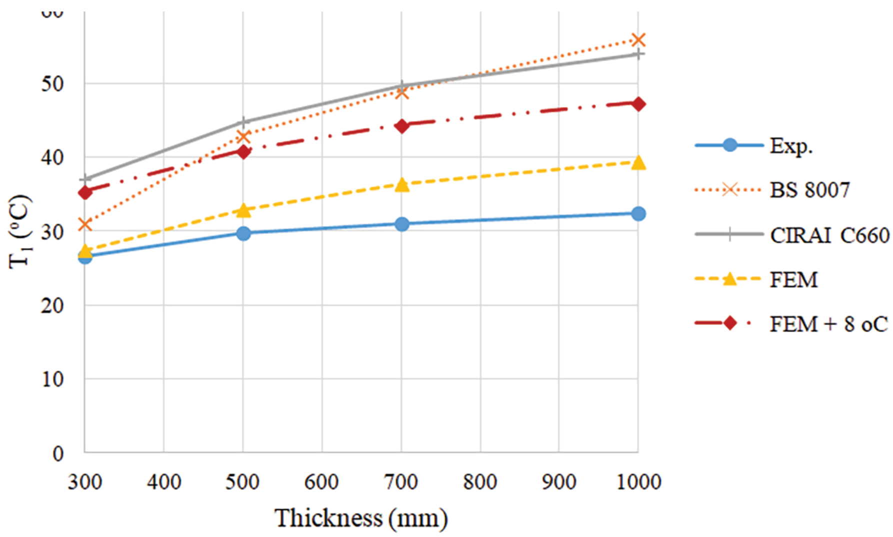

Figure 10 – FE Model Predictions for Nanayakkara and Wannigama (2003) Experiment

5.3 Parametric analysis

The validated numerical approach was used to predict T_1 values for 300 mm, 500 mm, 700 mm and 1000 mm thick concrete wall panels which were at five distinct mix compositions and at different formwork types. Considering the local conditions, the ambient and the initial concrete temperatures were assigned to be 30 °C and 32 °C, respectively. Also the formwork was assumed unremoved. Based on symmetry, only half wall thickness was modelled. Figure 11 illustrates the temperature outputs for two selected wall types. Note that the temperature is high at the wall interior (red colour) and low at the boundary (blue colour).

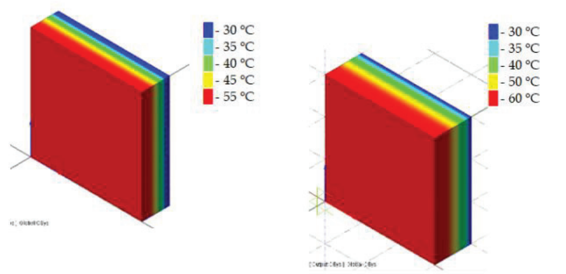

Figure 11 – Temperature Output: (a) 300 mm Wall; (b) 500 mm Wall

Table 4 presents the predicted T_1 values. Of note is that the table is presented in an order different to the mix numbers to facilitate comparisons across binder contents.

Figure 12 compares the numerically predicted temperature variation at the wall centre with the CIRIA C660 prediction for each wall thickness at the 349 kg/m^3 cement content and at 18 mm plywood formwork usage. It is highlighted that the numerical temperature prediction for each wall thickness is considerably lower than the CIRIA C660 predictions. For instance, the disparity is 26% and 22% for the wall thicknesses of 300 mm and 1000 mm, respectively. As previously highlighted, similar observations were also made by Nanayakkara and Wannigama [11] when their experimental T_1 values were compared with the code predictions, see Figures 2 and 10. When similar comparisons were made for the other concrete mixes, the disparity was observed to increase further with the cement richness of the mix. For instance, the CIRIA C660 prediction was 34% higher than the FE prediction for the 1000 mm thick wall with 560 kg/m^3 cement. Hence, this study verified the over conservativeness of T_1 obtained from the existing guidelines.

Based on the results in Table 4, Figure 13 shows the behaviour of T_1 with the binder content for the OPC mixes at the plywood formwork usage. It is also supplemented with the results of the 20% fly ash blended mix. Here, the equivalent binder content for this blended mix was computed to be 417 kg/m^3 as per the k-value concept introduced in BS EN 206-1: 2000 [23] and by assigning k = 0.4 for fly ash.

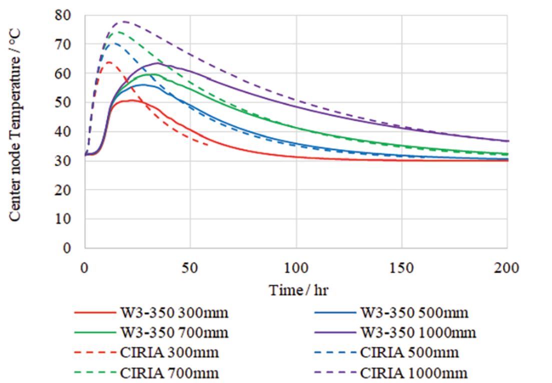

Figure 12 - Temperature Comparison for Wall Centre at 349 kg/m^3 Cement Content and 18 mm Plywood Formwork

Figure 13 shows that T_1 increases more rapidly for OPC mixes in the 349 - 420 kg/m^3 range than in the 420 - 560 kg/m^3 range. Even though not presented here, a similar behaviour was observed at the use of steel formwork. Another useful observation obtained from Figure 13 is that the use of fly ash has been able to reduce the temperature development significantly (in contrast to the OPC mix). To highlight the latter fact further, a comparison is made in Figure 14 where the T_1 outcomes (in Tables 4) are compared for the 420 kg/m^3 OPC mix and the two fly ash blended mixes at the plywood formwork usage. Of note is that, upon application of the k-value concept, the equivalent binder contents in 20% and 35% fly ash mixes became 417 kg/m^3 and 429 kg/m^3, respectively. Hence, the binder contents in the compared mixes were deemed reasonably similar to those in the OPC mix content of 420 kg/m^3.

Table 4 – Numerical T_1 Predictions

Wall thickness	T_1 (°C)									
	OPC 349 kg/m³ (M5-349)		OPC 420 kg/m³ (M2-420)		OPC 560 kg/m³ (M1-560)		Cement 379 kg/m³ Fly ash (20%) (M3-379-95)		Cement 353 kg/m³ Fly ash (35%) (M4-353-190)	
	Plywood	Steel	Plywood	Steel	Plywood	Steel	Plywood	Steel	Plywood	Steel
300 mm	20.7	14.8	30.0	21.7	34.7	25.4	24.7	18.0	21.9	16.1
500 mm	26.1	20.0	35.6	29.3	42.5	35.3	30.3	24.0	26.3	21.5
700 mm	29.7	24.6	39.0	34.6	46.5	44.2	34.0	28.9	29.6	25.2
1000 mm	33.5	29.9	41.8	39.7	49.7	47.3	37.3	34.5	32.6	30.1

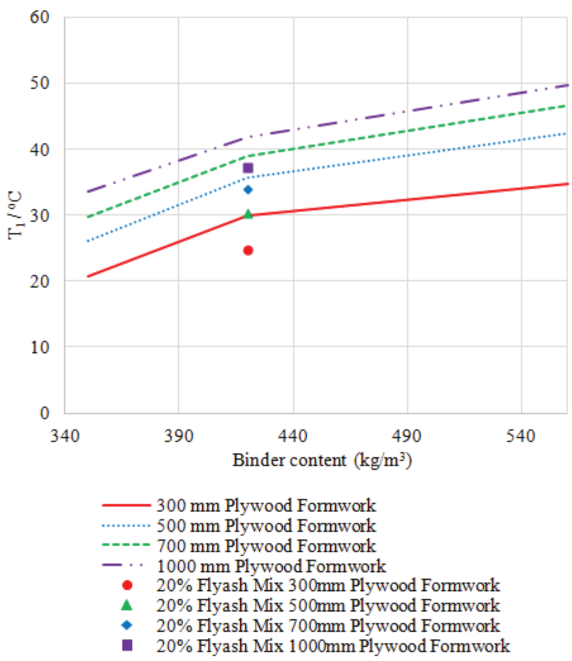

Figure 13 –T_1 vs. Binder Content

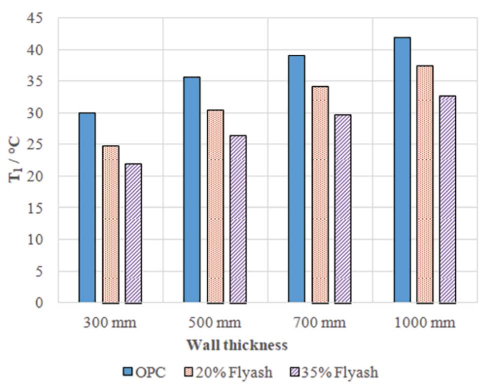

Figure 14 – Comparison of T_1 for OPC, 20% Fly Ash and 35% Fly Ash Mixes for an equivalent binder content ≈ 420 kg/m³

It is observed from Figure 14 that higher the fly ash composition, lower is T_1. By blending 20% and 35% of fly ash, the reduction of T_1 is as significant as 13% - 17% for 20% fly ash and 22% - 25% for 35% fly ash. This outcome can be deemed as an important quantitative observation in light of controlling of temperature for concrete structures via blending of supplementary cementitious materials (SCMs).

5.4 Recommendations for T_1

Assuming a linear variation of T_1 across the explored OPC regions (as shown in Figure 13), T_1 values for OPC compositions of 350, 400, 450, 500, and 550 kg/m³ for wall thicknesses between 300 - 1000 mm and for plywood and steel formwork, were obtained. Then, addressing the facts of: (a) observed 5.5 °C under-prediction for the mock-up experiment; and (b) current local practice of increasing the code predictions by 8 °C to account for the local climatic conditions, 8°C was added to the FE predictions and the values were rounded off. Similarly, Mataraaracchi et al. [12] highlighted that T_1 could vary about 7 - 12% depending on the chemical composition of the cement. Therefore, consideration of such a margin (8 °C) was deemed important. As highlighted in Figure 10, even with such augmentation, the FE based estimations are generally lower than the BS 8007 and CIRIA C660 values; hence, the use of the novel recommendations would still lead towards economical designs. Experimental validation of these recommendations is identified as a matter for future work. Also, it is worthwhile to explore the adiabatic behaviour of more mixes together with SCM blends in order to find more comprehensive recommendations for T_1.

Table 5 – Recommended T_1 (°C) Values

Form-work	OPC content kg/m³	Wall thickness (mm)			
		300	500	700	1000
18mm Plywood	350	29	34	38	42
	400	35	41	44	47
	450	39	45	49	52
	500	41	48	51	54
	550	42	50	54	57
Steel	350	23	28	33	38
	400	28	35	40	45
	450	31	39	45	49
	500	32	41	48	52
	550	33	43	52	55

6. Conclusions

Based on the findings of this study, the following conclusions can be drawn.

1. The validation of the FE model on experimental results was successful. The temperature behaviour, peak temperature and the time at the peak temperature of the two experiments were numerically predicted with a reasonable accuracy.

2. The peak temperature of the laboratory experiment was slightly over-predicted whereas that for the on-site experiment was slightly under-predicted. The incapability of the used numerical tool to account for the concrete maturity behaviour should be the reason for the former observation. The solar radiation could be a cause of additional temperature of the on-site experiment since that was not accounted in the FE simulation.

3. The numerical predictions highlighted that the recommended T_1 values in BS 8007 and in CIRIA C660 were too conservative for concrete walls. The observed disparity was in the range of 22% - 34%.

4. A series of T_1 was recommended for concrete walls of 300 mm – 1000 mm thickness, 350 kg/m³ to 550 kg/m³ cement content, and plywood and steel formwork usage. A conservative margin of 8 °C was considered in these recommendations.

5. By supplementing the concrete mixes with fly ash by 20% and 35%, significant reduction of T_1 could be achieved by about 15% and 23.5%, respectively.

6. Experimental validation of the recommended T_1 values is identified as a matter for future work. Furthermore, the experimentation into the concrete thermal parameters (utilised in the predictions) is also important.

Acknowledgements

The assistance provided by the technical staff of the Materials Laboratory of the University of Peradeniya is highly appreciated. Financial support provided by the INSEE 2019/2020 grant is also acknowledged.

References

1. Taylor, H. F. W., Famy, C. and Scrivener, K. L. (2001). ''Delayed Ettringite Formation''. *Cement and Concrete Research* 31(5): 683-693.

2. Neville, A. M. (2011). *Properties of Concrete*. 5th Ed., Pearson Education Limited, Harlow.

3. Bamforth, P. B. (2007). *CIRIA C660, Early-Age Thermal Crack Control in Concrete*. London.

4. Ballim, Y. (2004). "A Numerical Model and Associated Calorimeter for Predicting Temperature Profiles in Mass Concrete", *Cement and Concrete Composites* 26: 695 – 703.

5. Dissanayaka, D. M. M. and Yapa, H. D. (2021). "Numerical Prediction of Early Age Concrete Temperature via 3D Finite Difference Simulation", *Journal of the National Science Foundation of Sri Lanka,* 49(4): 539 – 550

6. Bobko, C. P., Zadeh, V. Z. and Seracino, R. (2015). "Improved Schmidt Method for Predicting Temperature Development in Mass Concrete", *ACI Materials Journal* 112 (4): 579 – 586.

7. Mosley, B., Bungey, J. and Hulse, R. (2012). *Reinforced Concrete Design to Eurocode 2*, 7th Ed., Palgrave Macmillan, Hampshire, UK.

8. BS 8007:1987: (1998). *Code of Practice for Design of Concrete Structures for Retaining Aqueous Liquids*. British Standard Institution, London.

9. SLS EN 1992-1-1: (2012). *Eurocode 2 – Design of Concrete Structures- Part 1-1: General Rules and Rules for Buildings*, Sri Lanka Standard Institution, Colombo.

10. SLS EN 1992-3: (2012) *Eurocode 2 – Design of Concrete Structures- Part 3: Liquid retaining and Containment Structures*, Sri Lanka Standard Institution, Colombo.

11. Nanayakkara S. M. A. & Wannigama W. R. K. (2003). "Experimental Investigation on Temperature Rise due to Heat of Hydration", *Annual Transactions of IESL*: 9-15.

12. Mataraarachchi, A. I. G. K., Nanayakkara S. M. A. and Asamoto, S. (2012). "Control of Thermal Cracking in Concrete Water Retaining Structures", *Proceedings of Second Annual Sessions, Society of Structural Engineers*, Sri Lanka, Colombo.

13. Morabito, P. & Barberis, F. (1993). "Measurement of Adiabatic Temperature Rise in Concrete", *Concrete 2000. Economic and Durable Construction through Excellence:* 749-759.

14. Ng, I. Y. T., Ng, P. L. & Kwan, A. K. H. (2009). "Effects of Cement and Water Contents on Adiabatic Temperature Rise of Concrete", *ACI Materials Journal* 106(1): 42-49.

15. Kwan, A. K. H., Ng, P. L., Ng, I. Y. T., Fung, W. W. S. & Chen, J. J. (2011b). "Adiabatic Temperature Rise of Pulverised Fuel Ash (PFA)", *Concrete. Advanced Materials Research* 168-170: 570-577.

16. Kwan, A. K. H., Ng, P. L., Fung, W. W. S., and Chen, J. J. (2011a). "Adiabatic Temperature Rise of Condensed Silica Fume (CSF) Concrete", *Advanced Materials Research* 261-263: 788-795.

17. Ng, P. L., Ng, I. Y. T., and Kwan, A. K. H. (2008). ''Heat Loss Compensation in Semi-Adiabatic Curing Test of Concrete''. *ACI Materials Journal* 105(1): 52-61.

18. Ng, P. L. & Kwan, A. K. H. (2012). ''Semi-adiabatic Curing Test with Heat Loss Compensation for Evaluation of Adiabatic Temperature Rise of Concrete''. *HKIE Transactions* 19(4):11-19.

19. Wasala, W. M. T. D. and Yapa H. D. (2017). ''Prediction of Temperature Development in Concrete using Semi-adiabatic Temperature Measurements'', *ENGINEER* L(3): 1-8.

20. Ballim, Y. & Graham, P. (2003). "A Maturity Approach to the Rate of Heat Evolution in Concrete", *Magazine of Concrete Research* 55: 249-256.

21. Soutsos, M, Hatzitheodorou A, Kanavaris, F. and Kwasny J. (2017). ''Effect of Temperature on the Strength Development of Mortar Mixes with GGBS and FA''. *Magazine of Concrete Research* 69(15**):** 787 – 80.

22. MIDAS FEA V 2.8. (2008). *Nonlinear and Detail FE Analysis System for Civil Structures, FEA Analysis and Algorithm Manual.*

23. BS EN 206-1: 2000. (2001). *Concrete. Specification, Performance, Production and Conformity*, British Standard Institution, London.